

PCDHGC3 hypermethylation as a potential biomarker of intestinal neuroendocrine carcinomas

Tamara Cubiella^{1,2}, Lucía Celada^{1,2} , Jaime San-Juan-Guardado^{1,2} , Raúl Rodríguez-Aguilar³, Álvaro Suárez-Priede^{1,2}, María Poch³, Francisco Dominguez³, Iván Fernández-Vega⁴, Pedro Montero-Pavón⁴, Mario F Fraga^{1,2,5,6}, Yoichiro Nakatani⁷, So Takata⁷, Shinichi Yachida⁷, Nuria Valdés^{6,8,9,10} and María-Dolores Chiara^{1,2,*} 

¹ Health Research Institute of the Principado de Asturias (ISPA), Oviedo, Spain

² Institute of Oncology of the Principado de Asturias, University of Oviedo, Oviedo, Spain

³ Department of Pathology, Hospital Universitario de Cabueñes, Gijón, Spain

⁴ Department of Pathology, Hospital Universitario Central de Asturias, Oviedo, Spain

⁵ Nanomaterials and Nanotechnology Research Center (CINN), Spanish National Research Council (CSIC), El Entrego, Spain

⁶ Spanish Biomedical Research Network in Rare Diseases (CIBERER), Madrid, Spain

⁷ Department of Cancer Genome Informatics, Graduate School of Medicine, Osaka University, Suita, Japan

⁸ Hospital Universitario Cruces, Bizkaia, Spain

⁹ Biobizkaia Health Research Institute, Bizkaia, Spain

¹⁰ CIBERDEM (Network of Biomedical Research in Diabetes), Madrid, Spain

*Correspondence to: M-D Chiara, Health Research Institute of the Principado de Asturias, Av. del Hospital Universitario, s/n, 33011 Oviedo, Spain.

E-mail: mdchiara.uo@uniovi.es

Abstract

Neuroendocrine neoplasms (NENs) encompass tumors arising from neuroendocrine cells in various organs, including the gastrointestinal tract, pancreas, adrenal gland, and paraganglia. Despite advancements, accurately predicting the aggressiveness of gastroenteropancreatic (GEP) NENs based solely on pathological data remains challenging, thereby limiting optimal clinical management. Our previous research unveiled a crucial link between hypermethylation of the protocadherin *PCDHGC3* gene and neuroendocrine tumors originating from the paraganglia and adrenal medulla. This epigenetic alteration was associated with increased metastatic potential and succinate dehydrogenase complex (SDH) dysfunction. Expanding upon this discovery, the current study explored *PCDHGC3* gene methylation within the context of GEP-NENs in a cohort comprising 34 cases. We uncovered promoter hypermethylation of *PCDHGC3* in 29% of GEP-NENs, with a significantly higher prevalence in gastrointestinal (GI) neuroendocrine carcinomas (NECs) compared with both pancreatic (Pan) NECs and neuroendocrine tumors (NETs) of GI and Pan origin. Importantly, these findings were validated in one of the largest multi-center GEP-NEN cohorts. Mechanistic analysis revealed that *PCDHGC3* hypermethylation was not associated with *SDH* mutations or protein loss, indicating an SDH-independent epigenetic mechanism. Clinically, *PCDHGC3* hypermethylation emerged as a significant prognostic factor, correlating with reduced overall survival rates in both patient cohorts. Significantly, whereas *PCDHGC3* hypermethylation exhibited a strong correlation with *TP53* somatic mutations, a hallmark of NEC, its predictive value surpassed that of *TP53* mutations, with an area under the curve (AUC) of 0.95 (95% CI 0.83–1.0) for discriminating GI-NECs from GI-NETs, highlighting its superior predictive performance. In conclusion, our findings position *PCDHGC3* methylation status as a promising molecular biomarker for effectively stratifying patients with GI-NENs. This discovery has the potential to advance patient care by enabling more precise risk assessments and tailored treatment strategies.

© 2024 The Authors. *The Journal of Pathology* published by John Wiley & Sons Ltd on behalf of The Pathological Society of Great Britain and Ireland.

Keywords: neuroendocrine carcinoma; methylation; epigenetic; protocadherins; *PCDHGC3*

Received 31 October 2023; Revised 9 February 2024; Accepted 3 April 2024

No conflicts of interest were declared.

Introduction

Neuroendocrine neoplasms (NENs) encompass several distinct entities that arise in various tissues, such as the pituitary, parathyroid, lung, skin, paraganglia, pancreas,

and gastrointestinal tract. Among them, gastroenteropancreatic neuroendocrine neoplasms (GEP-NENs) are the most frequent, originating from neuroendocrine cells located along the gastrointestinal tract (GI-NENs) and pancreas, pancreatic NENs (Pan-NENs) being the most

common type. GEP-NENs have become increasingly prevalent in recent years, affecting ~1–2 in 100,000 individuals annually. While most cases are sporadic, around 10% of Pan-NENs are associated with hereditary syndromes such as multiple endocrine neoplasia type I (MEN1), Von Hippel–Lindau syndrome (VHL), neurofibromatosis type I (NF1), and tuberous sclerosis complex (TSC) [1,2].

According to the 2022 WHO Classification of Neuroendocrine Neoplasms, GEP-NENs are classified into two main categories: well-differentiated neuroendocrine tumors (GEP-NETs) and poorly differentiated neuroendocrine carcinomas (GEP-NECs) [3]. NETs are further categorized as G1, G2, and G3 based on proliferation rate and Ki67 index, whereas NECs are inherently high grade with a high proliferation rate.

Clinically, distinguishing between GEP-NECs and GEP-NETs is crucial for accurate prognostication and optimal management of patients [4–7]. The WHO Classification of Endocrine and Neuroendocrine Tumors (2022) highlights *TP53* and *RB1* mutations as primary molecular markers for NEC. Nevertheless, there is a possibility of these mutations being present in a small proportion of G3 NETs as well [8]. *MEN1*, *DAXX*, and *ATRX* are the most frequently mutated genes in NETs [9], although more recent data suggest that their occurrence is lower than expected [10]. These findings indicate that NETs and NECs represent distinct malignancies on the molecular level, and that additional molecular characteristics may be used to differentiate and classify NECs from NETs when morphology is not sufficient.

Recent studies suggested that several adhesion molecules may play a key role in GEP-NEN tumorigenesis, although their involvement in tumor progression is less understood. For example, loss of E-cadherin expression has been identified as a key step in the development of Pan-NENs [11,12]. Cadherin-17 has also been shown to be involved in the proliferation and invasion of Pan-NENs [13]. Meanwhile, the role of cadherin-6 is still being explored, with preliminary evidence suggesting that it may promote tumor growth and invasion in G1-NENs [14,15]. The functions of other cadherins, such as the protocadherins, in GEP-NENs have not been previously explored.

Clustered protocadherins (cPCDHs) are cell adhesion molecules that belong to the cadherin family of adhesion proteins. They consist of 58 cell surface homophilic-adhesion molecules organized into three gene subclusters named alpha, beta, and gamma: *PCDHA@*, *PCDHB@*, and *PCDHG@*, respectively, located on human chromosome 5q31 [16]. The expression of *cPCDHs* is tightly regulated by complex mechanisms that involve stochastic promoter choice and DNA methylation [17]. These molecules are primarily expressed in the central nervous system, where they play crucial roles in various neurobiological processes [18]. However, some other tissues also maintain *cPCDH*.

Dysregulation of *PCDH* expression has been linked to several types of cancer, highlighting the broader

relationship between cadherin-mediated cell adhesion and oncogenesis [19–25]. Our previous research revealed that *PCDHGC3*, a member of the *PCDHG* family, is silenced through epigenetic mechanisms and may function as a tumor suppressor gene in paraganglioma and pheochromocytoma [25]. Its involvement in tumor progression has also been observed in colorectal cancer [21]. We have demonstrated that *PCDHGC3* has the potential to serve as a biomarker for identifying individuals with paragangliomas and pheochromocytomas carrying mutations in the succinate dehydrogenase B (*SDHB*) gene and having an increased risk of developing metastasis. However, the role of *PCDHGC3* in cancer, apart from colorectal cancer and paragangliomas or pheochromocytomas, remains largely unexplored. Therefore, in this current study, we aimed to expand upon previous findings by investigating *PCDHGC3* methylation in GEP-NENs. Our findings indicate that hypermethylation of *PCDHGC3* is present in GEP-NECs and is associated with a decreased overall survival rate. These results underscore the potential significance of investigating epigenetic alterations in neuroendocrine tumors and offer possibilities for a novel biomarker in the context of GEP-NENs.

Materials and methods

Tumor samples

Tumor tissues were obtained from 34 patients with GEP-NENs, diagnosed and treated between 2003 and 2017 at the Hospital Universitario Central de Asturias (Spain). Tumor samples included 34 primary tumors. In 12 cases, adjacent non-tumoral samples were available. Informed consent was obtained from each patient and the study was approved by the ethical committee of the hospital. The methods were carried out in accordance with the approved guidelines and the principles expressed in the Declaration of Helsinki. Clinical data were collected from patients' medical reports. Every tumor sample was reviewed by two qualified pathologists. Selected cases were studied applying tumor grading (G) according to the WHO classification of neuroendocrine neoplasms [3] and tumor staging (TNM) according to the Union for International Cancer Control/American Joint Committee on Cancer (UICC/AJCC), eighth edition [26].

Immunohistochemistry

FFPE human tumor tissue blocks were sectioned into 4- μ m slices and collected on poly-L-lysine-coated slides. To deparaffinize, rehydrate, and retrieve antigens, a high pH EnVision™ FLEX target retrieval solution was used for 20 min at 95 °C in a Dako PT link platform (Dako Denmark A/S, Glostrup, Denmark). Staining was performed using the Dako EnVision™ (Dako Denmark A/S) FLEX detection system with primary antibody against SDHB (rabbit anti-SDHB polyclonal, HPA002868, diluted 1:500; Sigma-Aldrich, St Louis, MO, USA) or p53

(FLEX Monoclonal Mouse Anti-Human p53 Protein Clone DO-7, Ready-to-Use; Agilent Dako, Santa Clara, CA, USA). To reduce assessment variability, immunohistochemistry for p53 was categorized as either 'pathogenic' (suggestive of *TP53* mutations) or 'non-pathogenic' (suggestive of wild-type *TP53*). More precisely, staining was considered 'pathogenic' in cases of negative or widespread over-expression in most cells, while sporadically weakly stained cells were interpreted as 'non-pathogenic' [27,28].

Targeted gene sequencing

The capture panel containing genes and regions of interest (*SDHB*, *SDHD*, *SDHC*, *SDHAF2*, *SDHA*, and *TP53*) was designed using the Agilent SureDesign tool (Agilent). The resulting FASTQ file analysis was performed using the Genome One platform certified with UNE-EN ISO 13485:2016 and IVD/CE-marking (Dreamgenics S.L., Oviedo, Spain). Raw FASTQ files were assessed using FastQC quality controls and Trimmomatic (<http://www.usadellab.org/cms/index.php?page=trimmomatic>) to remove bases, adapters, and other low-quality sequences. Each FASTQ file was aligned to the GRCh38/hg38 version of the human reference genome using BWA-mem [29]. The generation of sorted BAM files was performed using SAMtools (<http://www.htslib.org>), and the removal of optical and PCR duplicates was executed using Sambamba [30]. SNVs and Indels were identified through a combination of VarScan 2 (<http://varscan.sourceforge.net>) and a proprietary variant calling algorithm developed by Dreamgenics S.L. Variants were annotated using information from various functional databases (RefSeq, Pfam), population databases (dbSNP, 1000 Genomes, ESP6500, ExAC, gnomAD), clinical databases (ClinVar), *in silico* functional impact prediction (dbNSFP, dbSNV), and cancer-related information (ICGC).

DNA methylation analysis

The DNA methylation level of CpGs in the *PCDHGC3* gene was evaluated using bisulfite DNA modification, DNA amplification, and pyrosequencing. The DNA from tumor and normal tissues was extracted using the QIAamp DNA Kit (QIAGEN, Hilden, Germany). Bisulfite modification of the samples was performed using the EZ DNA Methylation-Gold™ Kit (Zymo Research, Irvine, CA, USA). Amplification of the region of interest was conducted with specific primers (5'-GGGATGAGGTAGAGATTGAATAG-3'; 5'-CCTCCAAACCTCTAAAACCATCTCA-3'). Pyrosequencing was carried out using the PyroMark Q24 Advanced System® (QIAGEN) with a specific primer (5'-GAGGTAGAGATTGAATAGT-3'). Primers were designed using the PyroMark assay designer (QIAGEN), focusing on the promoter region of the *PCDHGC3* gene TSS200 = 0–200 bases upstream of the transcription start site.

For data validation, we used a GEP-NEN cohort that had been previously published and analyzed using the

Infinium MethylationEPIC BeadChip (Illumina, San Diego, CA, USA) [31]. We used Illumina GenomeStudio software (version 2011.1) and retrieved AVG beta values for each CpG site, which ranged from 0 (unmethylated) to 1 (methylated). Our focus was on the promoter region of *PCDHGC3*, defined here as the genomic region located 200 bases upstream of the transcription start site of *PCDHGC3*.

Statistical analyses

Statistical analyses were performed using R version 3.5.2 (R Foundation for Statistical Computing, Vienna, Austria). ROC curves were used to evaluate the ability of the diagnostic test to distinguish between NETs and NECs. ROC curves were constructed by plotting the true-positive rate (sensitivity) against the false-positive rate (specificity) across various threshold values of the test results. The area under the ROC curve (AUC) was computed as a measure of the overall discriminative capacity of the test. Statistical analyses for the impact of *PCDHGC3 de novo* methylation on overall survival were performed using Kaplan–Meier analysis (log-rank analysis for statistical significance). We defined overall survival as the time that elapsed from the date of diagnosis to the date of death from any cause or last contact, whichever occurred first. $p < 0.05$ was defined as statistically significant.

Results

Clinicopathological characteristics of patients

The cohort consisted of 34 GEP-NENs along with 12 corresponding adjacent non-tumoral tissues. The mean age of the cohort was 63.2 ± 11.8 (range 41–87) years and the majority of the patients were male ($n = 19$, 55.9%). The most represented tumor site was the pancreas ($n = 15$, 44.1%), followed by the colorectum ($n = 8$, 23.5%), ileum–cecum–duodenum appendix ($n = 7$, 20.6%), and gastric ($n = 4$, 11.8%). Most patients ($n = 22$, 64.7%) had stage III–IV disease, and 12 (35.3%) had stage I–II disease. Patient follow-up was conducted in 30 patients over a median period of 55.5 (IQR 22.5–87) months. Table 1 summarizes the clinicopathological data of the included patients.

In accordance with the WHO classification [3], 14 (41.1%) tumors were categorized as NEC, with ten (71.4%) being GI-NEC and four (28.5%) being Pan-NEC. Additionally, 20 (58.5%) tumors were classified as NETs, comprising 11 (55.0%) Pan-NETs (five G1 and six G2) and nine (45%) GI-NETs (six G1, two G2, and one G3). Two cases of GI-NEN and one Pan-NEN were identified as mixed neuroendocrine and non-neuroendocrine neoplasms (MINENs).

De novo hypermethylation of *PCDHGC3* in GEP-NENs

The DNA methylation status of the *PCDHGC3* promoter region was assessed in a set of 12 non-tumor tissues,

Table 1. Relationships between *PCDHGC3* hypermethylation and *TP53* mutations and clinicopathological variables.

	<i>PCDHGC3</i> hypermethylation				<i>TP53</i> mutations			
	<i>n</i>	No	Yes	<i>p</i>	<i>n</i>	No	Yes	<i>p</i>
Age	34			0.165	32			0.343
<55 years		8	1			8	1	
>55 years		16	9			17	6	
Sex	34			0.529	32			0.649
Female		11	4			11	3	
Male		13	6			14	4	
Location	34			0.011	32			0.015
GI-NEN		10	9			12	7	
Pan-NEN		14	1			13	0	
T	28	No	Yes	0.185	29			0.485
T1		4	0			4	0	
T2		6	1			5	1	
T3		6	6			8	4	
T4		5	2			6	1	
N	31			0.1	30			0.068
N0		15	4			16	2	
N1		6	6			7	5	
M	32			0.024	30			0.326
M0		13	1			11	2	
M1		10	8			12	5	
NET/NEC	34			<0.0001	32			0.01
NET		19	1			18	1	
NEC		5	9			7	6	

consisting of two gastric, five colon, three small intestine, and two pancreas samples, showing no significant hypermethylation levels. The average methylation percentage was 3.8% (range 1.2–11.8%). In contrast, we identified substantial *de novo* hypermethylation of the *PCDHGC3* promoter, exceeding 12%, in 10 out of 34 (29%) GEP-NENs, as illustrated in Figure 1.

Interestingly, our study unveiled significant differences in the *PCDHGC3* methylation levels between NET and NEC. Specifically, *PCDHGC3* methylation was notably more prevalent in NEC cases, with 9 out of 14 cases (64%) exhibiting hypermethylation, than in NET cases, with only 1 out of 20 (5%) cases displaying hypermethylation ($p < 0.0001$). Further stratification by primary site revealed that this

methylation pattern was present in 9 out of 19 (47%) GI-NENs and 1 out of 15 (6.6%) Pan-NENs ($p = 0.0009$) (Figure 1 and Table 1). Furthermore, our analysis within the subset of GI-NEC cases revealed no preferential hypermethylation across different anatomical locations, encompassing the stomach, colon, or ileum. In MINENs, *PCDHGC3* hypermethylation was detected in two of the three tumors. The molecular–clinical associations remained consistent when these tumors were excluded from the analysis.

No relationship was observed between *PCDHGC3* hypermethylation levels and sex, tumor size, or lymph node metastasis (Table 1). While *PCDHGC3* hypermethylation demonstrated a significant association with distant metastases ($p = 0.024$), the analysis yielded

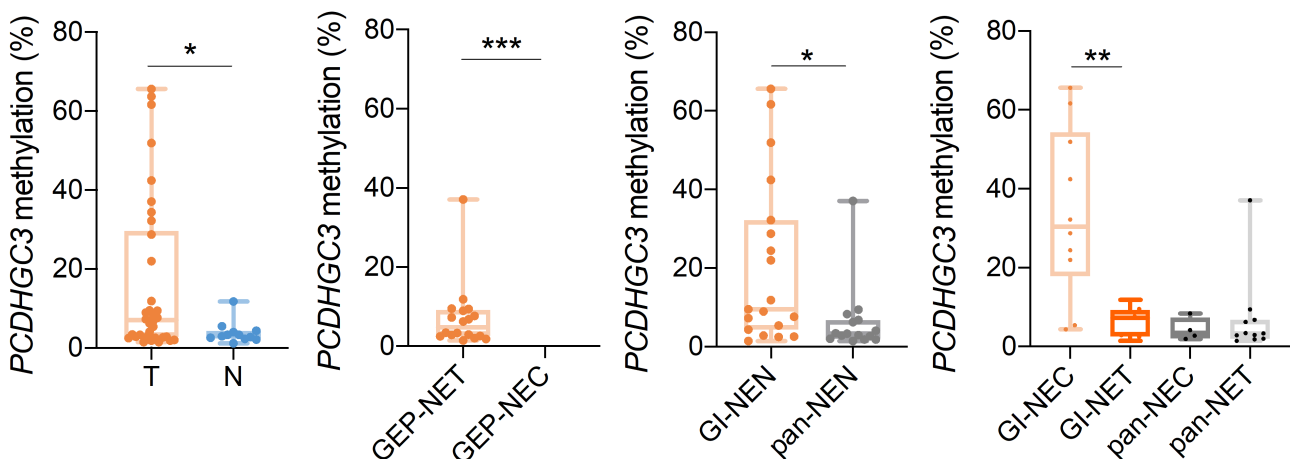


Figure 1. *PCDHGC3* promoter methylation in GEP-NENs. Graphic representations of the percentages of *PCDHGC3* promoter methylation in tumoral (T) and non-tumoral (N) samples (left) or in GEP-NENs, stratified as NET or NEC, and categorized according to the tissue of origin.

no statistical significance when confined to NEC or NET cases ($p = 0.5$ and $p = 0.437$, respectively).

Validation of *de novo* hypermethylation of *PCDHGC3* in GI-NECs

Significantly, our findings underwent independent validation using a previously reported large-scale cohort that included 23 GI-NECs and 40 Pan-NENs (comprising 28 NET and 12 NEC cases). The data confirmed the prevailing presence of *PCDHGC3* hypermethylation (with beta values exceeding 40%) in NEC cases (10 out of 35 cases, 29%) in contrast with NET cases (1 out of 28 cases, 3.6%) ($p = 0.009$). Additionally, a higher incidence, albeit not statistically significant, was observed in GI-NEC cases (8 out of 23 cases, 34.8%) compared with Pan-NEC cases (2 out of 12, 16%). However, given that our exploratory and validation datasets are enriched in gastrointestinal tumors, it remains uncertain whether *PCDHGC3* methylation truly distinguishes between GI-NEC and Pan-NEC cases.

Our prior study documented the methylation-driven upregulation of the *SOX2* transcription factor, recognized for its involvement in neuroendocrine differentiation within GEP-NECs. Upon evaluating the hypermethylation status of both *SOX2* and *PCDHGC3* in the validation cohort, a significant correlation was observed ($r = 0.390$, $p = 0.002$) (Figure 2). Nonetheless, it is important to note that not all tumors exhibiting *SOX2* methylation displayed concurrent *PCDHGC3* methylation, implying the involvement of both shared and distinct epigenetic regulatory mechanisms.

PCDHGC3 methylation is not associated with genetic loss of function of *SDH* genes

Targeted exome sequencing of *SDH* genes showed that there were no mutations in *SDHB*, *SDHC*, *SDHD*, *SDHA*, and *SDHAF2* in any of the GEP-NENs. *SDH*-deficient tumors have also been associated with the epigenetic silencing of the *SDHC* gene through promoter hypermethylation. However, upon analyzing the DNA promoter methylation of the *SDHC* gene in tumors

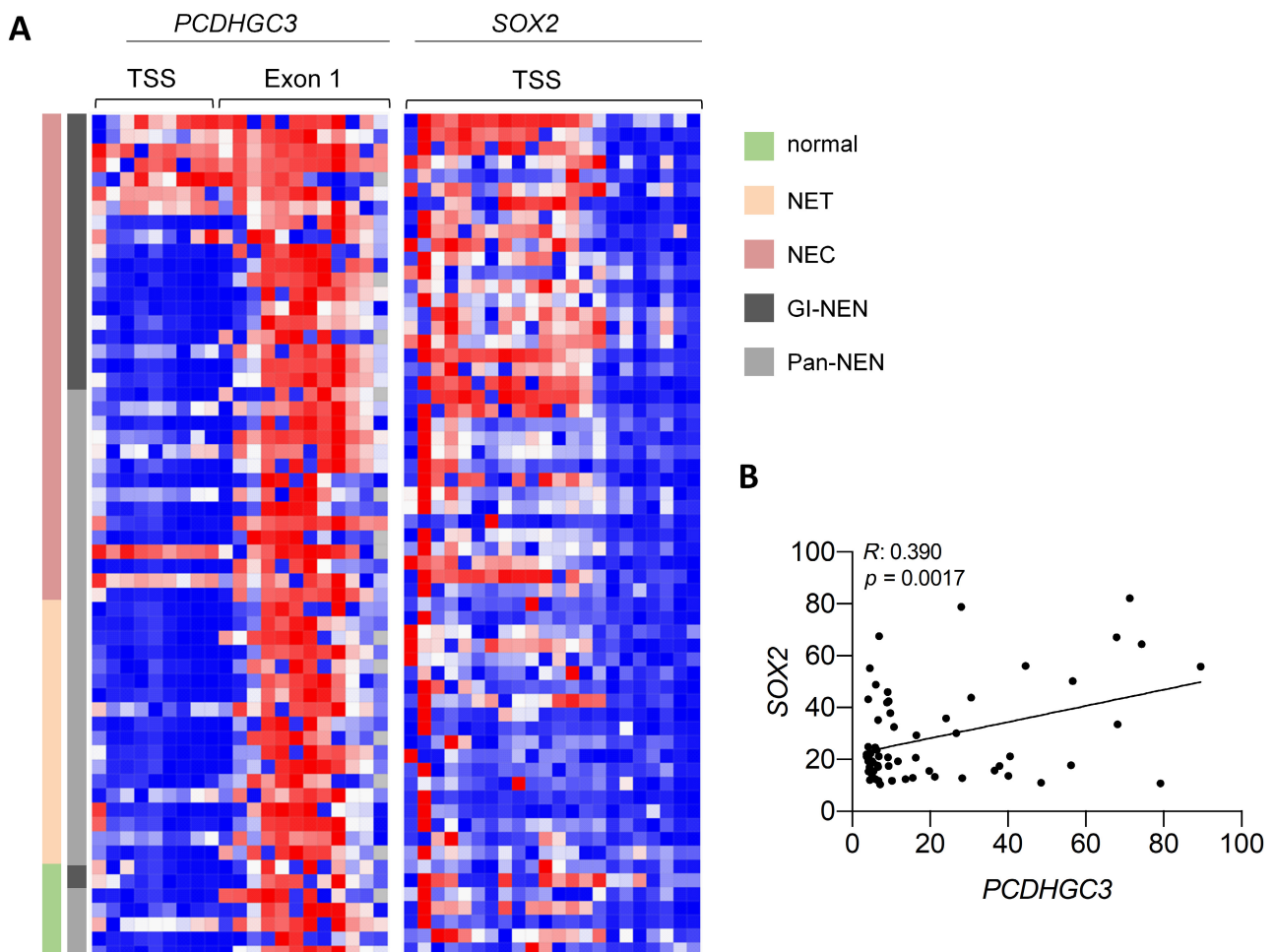


Figure 2. Validation of *PCDHGC3* methylation data. (A) Heatmap representation of the transcription start site (TSS) and exon 1 sequences of *PCDHGC3* (left) and the TSS of *SOX2* (right). Each column represents a probe set from the validation cohort, and each row represents a sample. (B) Scatterplot depicting the correlation between methylation levels of the *PCDHGC3* and *SOX2* genes within the validation cohort. Median beta values of each probe situated in the TSS regions of the specified genes were used. Methylation data are displayed on a scale of 0 (no methylation) to 100 (full methylation).

carrying *PCDHGC3* methylation, we found no evidence of *SDHC* hypermethylation. Additionally, *SDHB* immunohistochemistry indicated the presence of an intact *SDH* complex (Figure 3). It is essential to note that the loss of *SDHB* protein serves as an indicator of inactivating mutations or deletions in any of the *SDH* genes. Consequently, based on these findings, we can conclude that *PCDHGC3* methylation in GEP-NENs is not associated with *SDH* loss of function, as observed in paraganglioma and pheochromocytoma.

PCDHGC3 methylation is associated with *TP53* mutations in GEP-NENs

TP53 sequencing analysis identified inactivating mutations in 21% (7 out of 32) of the analyzed tumors. In line with previous reports, *TP53* mutations were significantly associated with NEC originating in the GI tract. Specifically, all (7 out of 7) *TP53*-mutated GEP-NENs were of GI origin, and six of them had been diagnosed as NEC ($p = 0.015$, Table 1).

The data were corroborated by immunohistochemical analysis of p53 (Figure 4). Among the cases with p53 overexpression, all had *TP53* non-synonymous mutations, whereas the only case with the absence of p53 immunostaining had a *TP53* deletion.

As expected, *PCDHGC3* hypermethylation was significantly associated with *TP53* mutation ($p = 0.001$) or positive p53 immunostaining ($p = 0.034$) (Figure 4 and Table 1). This association aligns with the knowledge that *TP53* mutation is predominantly found in NEC. Nevertheless, among cases with *PCDHGC3* methylation, the absence of *TP53* mutations or negative p53 immunostaining was found in 40% and 55% of cases, respectively. In addition, *PCDHGC3* hypermethylation was not associated with *TP53* mutations in our validation cohort ($p = 0.109$). Collectively, these data suggest that dysfunction of p53 is not casually related to *PCDHGC3* hypermethylation.

Relationships between *PCDHGC3* methylation and overall survival

We collected follow-up data from 30 patients with a median follow-up of 55.5 months. Among them, 14 patients (41.2%) died of the disease after a median time of 38.7 ± 35.6 months from diagnosis. Kaplan–Meier survival curve analysis revealed no significant differences in survival time between patients with GI-NENs and Pan-NENs ($p = 0.793$). Patients with NETs exhibited a more favorable overall survival (OS) compared with those with NEC ($p = 0.037$).

Furthermore, our analysis revealed that patients with *PCDHGC3* methylation had a significantly shorter OS in comparison to those without methylation (median 106 versus 29.6 months, $p = 0.002$), as depicted in Figure 5. Similarly, patients with *TP53* mutation showed a reduced OS compared with those without mutations (median 110 versus 24 months; $p < 0.0001$). Exclusion of MINENs from the analysis did not significantly modify the results ($p < 0.0001$ for both *PCDHGC3* hypermethylation and *TP53* mutation). Furthermore, these associations remained consistent in the validation cohort as well, with *PCDHGC3* hypermethylation and *TP53* mutations both being correlated with shorter overall survival ($p = 0.011$ and $p = 0.012$, respectively).

Evaluating the diagnostic potential of *PCDHGC3* hypermethylation and *TP53* mutations in GEP-NECs versus GEP-NETs

Given the higher prevalence of both *PCDHGC3* methylation and *TP53* mutations in GEP-NECs compared with GEP-NETs, we assessed their predictive value for distinguishing these tumor entities. *PCDHGC3* methylation exhibited a sensitivity of 64.3%, a specificity of 95%, and a positive predictive value of 90% in distinguishing GEP-NECs from GEP-NETs. In contrast, *TP53* mutations demonstrated a sensitivity of 46.2%, a specificity of 94.7%, and a positive predictive

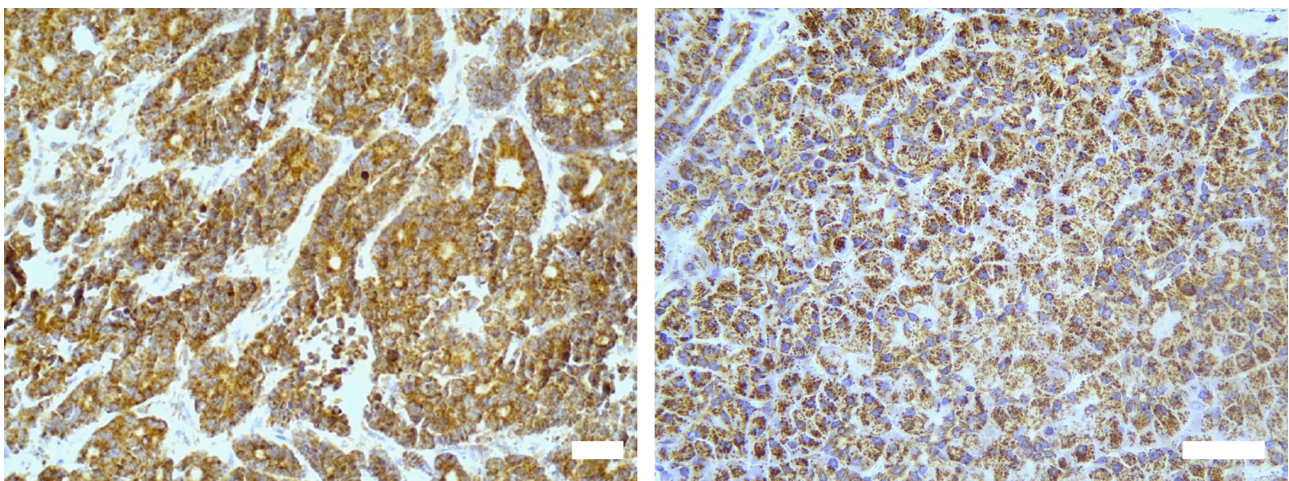


Figure 3. Immunohistochemistry for *SDHB* as a marker of *SDHA*, *SDHB*, *SDHC*, and *SDHD* gene mutations. Representative immunohistochemical images of *SDHB* in two GEP-NEN samples. Both samples exhibit granular and intense staining, irrespective of high *PCDHGC3* methylation levels (left) or the absence of such methylation (right). Scale bars: 50 μm .

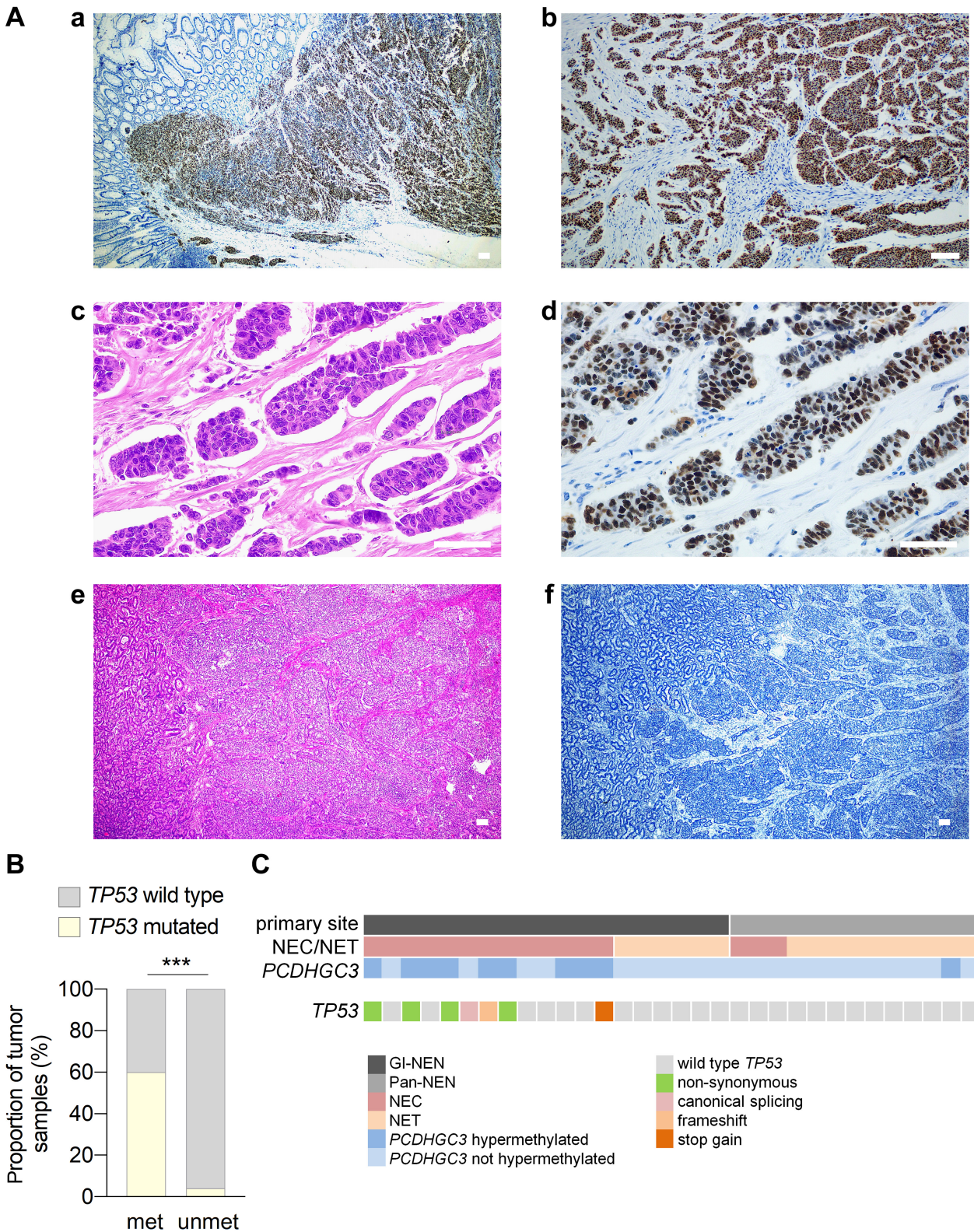


Figure 4. Relationship between *PCDHGC3* methylation and *TP53* mutation. (A) Representative images of p53 immunohistochemistry (a, b, d, f) and hematoxylin staining (c, e) in two independent NEC tumors that carry either a non-synonymous Tyr205Asp *TP53* mutation (a–d) or a frameshift Asp48Argfs*76 *TP53* mutation (e, f). (B) Bar chart displaying the relationship between *TP53* mutations and the presence (met) or absence (unmet) of *PCDHGC3* methylation. (C) Characteristics of the cohort of tumors and identified *PCDHGC3* methylation status and *TP53* somatic mutations. ****p* < 0.001.

value of 85.7% in distinguishing GEP-NECs from GEP-NETs.

In the context of GI-NECs, *PCDHGC3* hypermethylation achieved a sensitivity of 90%, a specificity of 100%, and a

positive predictive value of 100% in distinguishing NECs from NETs. *TP53* mutations yielded a sensitivity of 60%, a specificity of 88.9%, and a positive predictive value of 85.7% in distinguishing GI-NECs from GI-NETs.

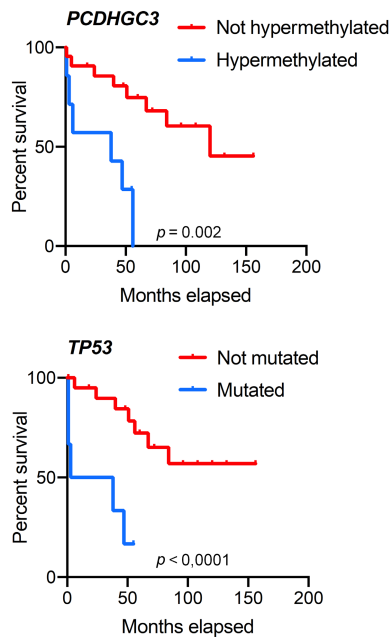


Figure 5. Prognostic value of *PCDHGC3* methylation and *TP53* mutation. Kaplan–Meier curves for overall survival according to levels of *PCDHGC3* hypermethylation and *TP53* mutation. The *PCDHGC3* data were divided as low and high according to their mean values (16.4%). *p* values were calculated using the Kaplan–Meier test.

As shown in Figure 6, the calculated areas under the curve (AUCs) for *PCDHGC3* methylation levels, with a cut-off value of 16.9%, were 79.11 (95% CI 62.1–96.0) for distinguishing GEP-NECs from GEP-NETs and 95.0 (95% CI 83.7–100) for distinguishing GI-NECs from GI-NETs. Conversely, the AUCs for *TP53* mutations were 70.4 (95% CI 55.4–85.4) for distinguishing GEP-NECs from GEP-NETs and 74.4 (95% CI 51.4–97.6) for distinguishing GI-NECs from GI-NETs. When MINENs were excluded from the analysis, the AUCs for *PCDHGC3* methylation levels were 73.9% (95% CI 54.1–93.6) for distinguishing GEP-NECs from GEP-NETs and 92.9 (95% CI 76.9–100) for distinguishing GI-NECs from GI-NETs. In contrast, for *TP53* mutations, the AUCs were 62.4% (95% CI 39.5–85.2) and 65.9 (95% CI 37.5–94.3) for distinguishing GEP-NECs from GEP-NETs or GI-NECs from GI-NETs, respectively. These findings underscore the potential of *PCDHGC3* methylation as a putative diagnostic marker, surpassing *TP53* mutations, to effectively differentiate between GEP-NEC and GEP-NET cases.

Discussion

In this study, we uncovered the presence of *PCDHGC3* promoter hypermethylation in GEP-NENs. Notably, *PCDHGC3* hypermethylation is rarely encountered in GEP-NETs from any location and in pancreatic NEC. These findings may hold significant implications for the diagnosis, prognosis, and treatment of affected patients.

The distinction between NETs and NECs can be a complex and challenging process when relying solely on histopathology [6–8]. This distinction is of paramount significance because these two tumor types are associated with differing prognoses and treatment benefits. To address this, the WHO classification aims to incorporate molecular parameters. In this context, our study highlights the significance of *PCDHGC3* promoter hypermethylation as a defining feature in approximately 40% of all GI-NECs, providing a clear demarcation from NETs. While mutations or inactivation of the *TP53* gene have been considered a hallmark of NECs [32], absent in NETs, our data now provide a more valuable tool than *TP53* for distinguishing between these entities. Notably, we found that *PCDHGC3* hypermethylation outperforms *TP53* mutations in effectively differentiating GI-NECs from GI-NETs. This epigenetic modification can enhance the categorization of challenging NEN cases, leading to improved patient management and more informed treatment decisions. However, since the most pressing need is to differentiate between NET G3 and NEC and considering that our cohort includes only one patient with G3-NET, further studies are warranted to fully evaluate the diagnostic potential of this epigenetic trait.

In this study, we observed that *PCDHGC3* hypermethylation predominantly occurred in NECs of gastrointestinal origin, while only a minority of Pan-NECs exhibited this alteration. This observation aligns with previous studies implicating aberrant DNA methylation as a crucial mechanism in GI-NEC progression [31,33]. However, it is important to acknowledge that this result may be biased due to the higher prevalence of GI-NENs (78%) compared with Pan-NENs (29%) in the patient cohorts. Therefore, further investigations with larger sample sizes and diverse cohorts are warranted to confirm our findings and explore potential tissue-specific differences in *PCDHGC3* methylation patterns.

Mechanistically, we found that SDH deficiency is largely absent in GEP-NENs, suggesting that it is not a contributing factor to *PCDHGC3* methylation in NEC, in contrast to paraganglioma and pheochromocytoma [25]. We also explored the possibility that *PCDHGC3* promoter methylation may be part of a broader hypermethylation pattern affecting genes involved in neuroendocrine differentiation. In the validation cohort used in this study, hypermethylation of *SOX2*, a transcription factor linked to neuroendocrine differentiation, had been found in GEP-NEC cases [31]. However, despite the correlation between these two epigenetic alterations, there is no distinct overlap between *SOX2* and *PCDHGC3* methylation patterns in these samples. Taken together, these results suggest that *PCDHGC3* methylation possesses shared features as well as distinctive attributes, setting it apart as a unique epigenetic alteration in GI-NEC.

While our study has limitations due to the relatively small sample size of the discovery cohort, the findings were substantiated by the inclusion of a significantly larger validation cohort. Furthermore, our results align with previous research, including our own, underscoring

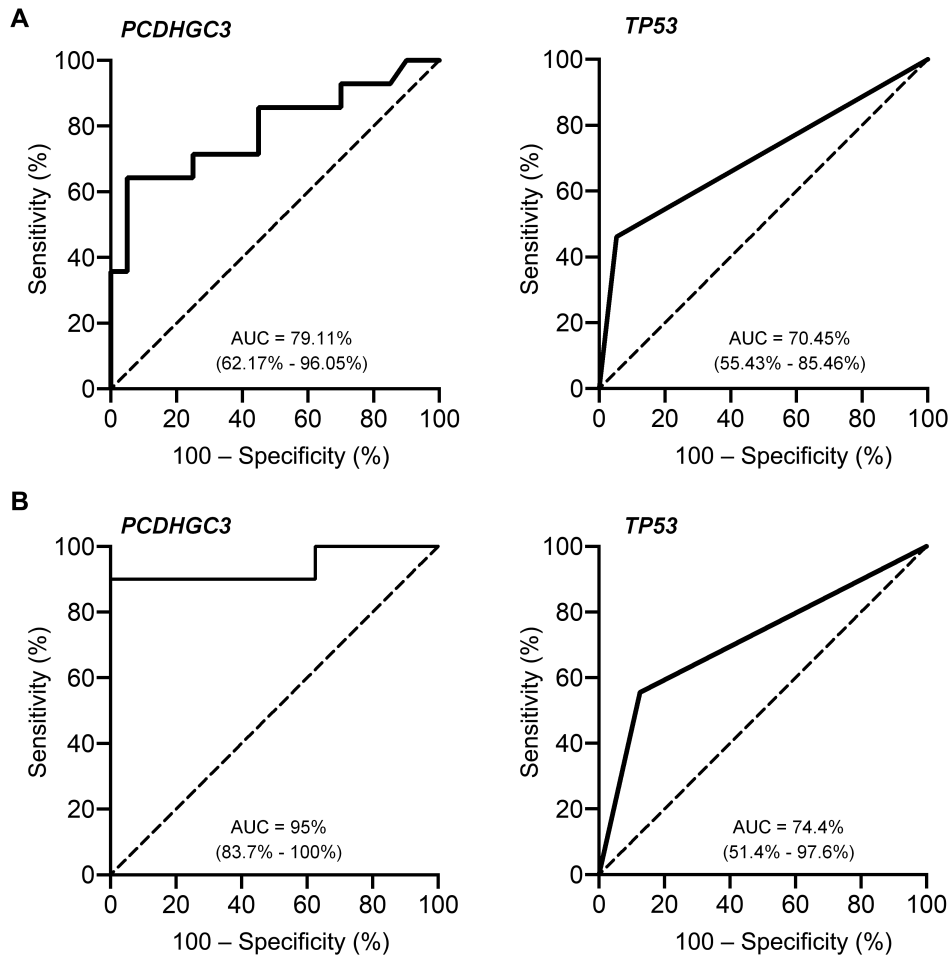


Figure 6. Receiver operating characteristic (ROC) curve analysis for *PCDHGC3* and *TP53* in NEC versus NET prediction. (A and B) ROC curves assessing the predictive performance of *PCDHGC3* methylation and *TP53* mutations for distinguishing between GEP-NETs and GEP-NECs (A) and between GI-NETs and GI-NECs (B).

the significance of *PCDHGC3* methylation in cancer progression [22,25,34]. We have previously reported the epigenetic silencing of *PCDHGC3* in two other types of neuroendocrine tumors, paraganglioma and pheochromocytoma [25]. Notably, this epigenetic trait was progressively amplified during the transition from benign to metastatic tumor cells, leading to increased cell proliferation and migration. Furthermore, Dallosso *et al* have suggested that *PCDHGC3* promoter hypermethylation may serve as a pivotal driver in the colorectal adenoma-carcinoma transition [22]. Significantly, *PCDHGC3* methylation has been linked to the activation of druggable target pathways, such as mTOR and WNT signaling [22,35]. These collective findings are particularly relevant due to their potential to transform treatment approaches for specific types of cancers. Traditionally, the treatment decisions for GEP-NENs have largely relied on histopathological and clinical features. Our results may contribute to the development of tailored therapies based on the unique epigenetic profile of each GEP-NEN, with the potential to enhance treatment efficacy while minimizing adverse effects.

In conclusion, our study underscores the clinical relevance of *PCDHGC3* hypermethylation as a distinguishing

feature of GEP-NECs, signaling their more aggressive nature compared with NETs. This insight opens exciting avenues for personalized, molecularly-driven therapies in the challenging landscape of GI-NECs, offering hope for improved outcomes and more effective treatment strategies.

Acknowledgements

This research was funded by Instituto de Salud Carlos III through the project PI20/01754 (co-funded by the European Regional Development Fund/European Social Fund 'A way to make Europe'/'Investing in your future') and the Principado de Asturias and European Regional Development Fund through the project IDI/2021/00079. We want to particularly acknowledge the patients and the Biobank of the Principality of Asturias (BioPA) (National Registry of Biobanks B.0000827) (PT23/00077 funded by ISCIII and co-funded by the European Union) integrated in the Platform ISCIII Biobanks and Biomodels for their collaboration. LC thanks The Spanish Ministerio de

Ciencia, Innovación y Universidades for a FPU predoctoral contract. TC and JS-JG thank Consejería de Ciencia, Innovación y Universidad (Principado de Asturias) for Severo-Ochoa predoctoral contracts.

Author contributions statement

M-DC was responsible for conceptualization. TC, LC, JS-JG, AS-P, RR-A, MP and FD were responsible for the methodology. M-DC, NV, TC, IF-V, PM-P, MFF, SY, YN and ST carried out the formal analysis. M-DC, NV and TC wrote the manuscript. TC, M-DC, NV, MFF, SY, YN and ST reviewed and edited the manuscript. M-DC and NV acquired funding. All authors have read and agreed to the published version of the manuscript.

Data availability statement

The data that support the findings of this study are available from the corresponding author upon reasonable request.

References

- Shen X, Wang X, Lu X, *et al.* Molecular biology of pancreatic neuroendocrine tumors: from mechanism to translation. *Front Oncol* 2022; **12**: 967071.
- Giandomenico V, Modlin IM, Pontén F, *et al.* Improving the diagnosis and management of neuroendocrine tumors: utilizing new advances in biomarker and molecular imaging science. *Neuroendocrinology* 2013; **98**: 16–30.
- Rindi G, Mete O, Uccella S, *et al.* Overview of the 2022 WHO classification of neuroendocrine neoplasms. *Endocr Pathol* 2022; **33**: 115–154.
- Thomas KEH, Voros BA, Boudreaux JP, *et al.* Current treatment options in gastroenteropancreatic neuroendocrine carcinoma. *Oncologist* 2019; **24**: 1076–1088.
- Milione M, Maisonneuve P, Grillo F, *et al.* Ki-67 index of 55% distinguishes two groups of bronchopulmonary pure and composite large cell neuroendocrine carcinomas with distinct prognosis. *Neuroendocrinology* 2021; **111**: 475–489.
- Sorbye H, Baudin E, Borbath I, *et al.* Unmet needs in high-grade gastroenteropancreatic neuroendocrine neoplasms (WHO G3). *Neuroendocrinology* 2019; **108**: 54–62.
- Uccella S, La Rosa S, Metovic J, *et al.* Genomics of high-grade neuroendocrine neoplasms: well-differentiated neuroendocrine tumor with high-grade features (G3 NET) and neuroendocrine carcinomas (NEC) of various anatomic sites. *Endocr Pathol* 2021; **32**: 192–210.
- Umetsu SE, Kakar S, Basturk O, *et al.* Integrated genomic and clinicopathologic approach distinguishes pancreatic grade 3 neuroendocrine tumor from neuroendocrine carcinoma and identifies a subset with molecular overlap. *Mod Pathol* 2023; **36**: 100065.
- Jiao Y, Shi C, Edil BH, *et al.* DAXX/ATRAX, MEN1, and mTOR pathway genes are frequently altered in pancreatic neuroendocrine tumors. *Science* 2011; **331**: 1199–1203.
- Venizelos A, Elvebakken H, Perren A, *et al.* The molecular characteristics of high-grade gastroenteropancreatic neuroendocrine neoplasms. *Endocr Relat Cancer* 2021; **29**: 1–14.
- Li CC, Xu B, Hirokawa M, *et al.* Alterations of E-cadherin, alpha-catenin and beta-catenin expression in neuroendocrine tumors of the gastrointestinal tract. *Virchows Arch* 2002; **440**: 145–154.
- Yonemori K, Kurahara H, Maemura K, *et al.* Impact of Snail and E-cadherin expression in pancreatic neuroendocrine tumors. *Oncol Lett* 2017; **14**: 1697–1702.
- Snow AN, Mangray S, Lu S, *et al.* Expression of cadherin 17 in well-differentiated neuroendocrine tumours. *Histopathology* 2015; **66**: 1010–1021.
- Edfeldt K, Björklund P, Åkerström G, *et al.* Different gene expression profiles in metastasizing midgut carcinoid tumors. *Endocr Relat Cancer* 2011; **18**: 479–489.
- Carr JC, Boese EA, Spanheimer PM, *et al.* Differentiation of small bowel and pancreatic neuroendocrine tumors by gene-expression profiling. *Surgery* 2012; **152**: 998–1007.
- Mountoufaris G, Canzio D, Nwakeze CL, *et al.* Writing, reading, and translating the clustered protocadherin cell surface recognition code for neural circuit assembly. *Annu Rev Cell Dev Biol* 2018; **34**: 471–493.
- Hirayama T, Yagi T. Regulation of clustered protocadherin genes in individual neurons. *Semin Cell Dev Biol* 2017; **69**: 122–130.
- Flaherty E, Maniatis T. The role of clustered protocadherins in neurodevelopment and neuropsychiatric diseases. *Curr Opin Genet Dev* 2020; **65**: 144–150.
- Shan M, Su Y, Kang W, *et al.* Aberrant expression and functions of protocadherins in human malignant tumors. *Tumour Biol* 2016; **37**: 12969–12981.
- Novak P, Jensen T, Oshiro MM, *et al.* Agglomerative epigenetic aberrations are a common event in human breast cancer. *Cancer Res* 2008; **68**: 8616–8625.
- Dallosso AR, Øster B, Greenhough A, *et al.* Long-range epigenetic silencing of chromosome 5q31 protocadherins is involved in early and late stages of colorectal tumorigenesis through modulation of oncogenic pathways. *Oncogene* 2012; **31**: 4409–4419.
- Dallosso AR, Hancock AL, Szemes M, *et al.* Frequent long-range epigenetic silencing of protocadherin gene clusters on chromosome 5q31 in Wilms' tumor. *PLoS Genet* 2009; **5**: e1000745.
- Miyata T, Sonoda K, Tomikawa J, *et al.* Genomic, epigenomic, and transcriptomic profiling towards identifying omics features and specific biomarkers that distinguish uterine leiomyosarcoma and leiomyoma at molecular levels. *Sarcoma* 2015; **2015**: 412068.
- Wang K-H, Lin C-J, Liu C-J, *et al.* Global methylation silencing of clustered proto-cadherin genes in cervical cancer: serving as diagnostic markers comparable to HPV. *Cancer Med* 2015; **4**: 43–55.
- Bernardo-Castañeira C, Valdés N, Celada L, *et al.* Epigenetic deregulation of protocadherin PCDHGC3 in pheochromocytomas/paragangliomas associated with SDHB mutations. *J Clin Endocrinol Metab* 2019; **104**: 5673–5692.
- Amin MB, Greene FL, Edge SB, *et al.* The Eighth Edition AJCC Cancer Staging Manual: continuing to build a bridge from a population-based to a more 'personalized' approach to cancer staging. *CA Cancer J Clin* 2017; **67**: 93–99.
- Yemelyanova A, Vang R, Kshirsagar M, *et al.* Immunohistochemical staining patterns of p53 can serve as a surrogate marker for TP53 mutations in ovarian carcinoma: an immunohistochemical and nucleotide sequencing analysis. *Mod Pathol* 2011; **24**: 1248–1253.
- Li J, Wang J, Su D, *et al.* p53 immunohistochemistry patterns are surrogate biomarkers for TP53 mutations in gastrointestinal neuroendocrine neoplasms. *Gastroenterol Res Pract* 2021; **2021**: 2510195.

29. Li H, Durbin R. Fast and accurate short read alignment with Burrows-Wheeler transform. *Bioinformatics* 2009; **25**: 1754–1760.
30. Tarasov A, Vilella AJ, Cuppen E, et al. Sambamba: fast processing of NGS alignment formats. *Bioinformatics* 2015; **31**: 2032–2034.
31. Yachida S, Totoki Y, Noë M, et al. Comprehensive genomic profiling of neuroendocrine carcinomas of the gastrointestinal system. *Cancer Discov* 2022; **12**: 692–711.
32. Ali AS, Grönberg M, Federspiel B, et al. Expression of p53 protein in high-grade gastroenteropancreatic neuroendocrine carcinoma. *PLoS One* 2017; **12**: e0187667.
33. Colao A, de Nigris F, Modica R, et al. Clinical epigenetics of neuroendocrine tumors: the road ahead. *Front Endocrinol (Lausanne)* 2020; **11**: 604341.
34. Feldheim J, Wend D, Lauer MJ, et al. Protocadherin gamma C3 (PCDHGC3) is strongly expressed in glioblastoma and its high expression is associated with longer progression-free survival of patients. *Int J Mol Sci* 2022; **23**: 8101.
35. Gabbert L, Dilling C, Meybohm P, et al. Deletion of protocadherin gamma C3 induces phenotypic and functional changes in brain microvascular endothelial cells *in vitro*. *Front Pharmacol* 2020; **11**: 590144.